Rapid synthesis of Ag@Ni core-shell nanoparticles using a microwave-polyol method

Tsuji, Masaharu
Department of Applied Science for Electronics and Materials, Graduate School of Engineering Sciences, Kyushu University

Hikino, Sachie
Institute for Materials Chemistry and Engineering, Kyushu University

Matsunaga, Mika
Institute for Materials Chemistry and Engineering, Kyushu University

Sano, Yoshiyuki
R and D Department, DIC Corporation

他

https://hdl.handle.net/2324/26031

Rapid synthesis of Ag@Ni core-shell nanoparticles using a microwave-polyol method

Masaharu Tsuji*[a,b], Sachie Hikino[a], Mika Matsunaga[a], Yoshiyuki Sano[c],

Tomoe Hashizume[d], Hirofumi Kawazumi[d]

[a] *Institute for Materials Chemistry and Engineering, Kyushu University, Kasuga 816-8580,*

Japan

[b] *Department of Applied Science for Electronics and Materials, Graduate School of*

 Engineering Sciences, Kyushu University, Kasuga 816-8580, Japan

[c] *R&D Department, DIC Corporation, Sakura 285-8668, Japan*

[d] *Department of Biological and Environmental Chemistry, School of Humanity-oriented Science and Technology, Kinki University, Iizuka 820-8555, Japan*

ABSTRACT

Mixtures of $AgNO_3$ and $NiSO_4 \cdot 6H_2O$, $NiCl_2 \cdot 6H_2O$, or $Ni(NO_3)_2 \cdot 6H_2O$ were reduced in

ethylene glycol (EG) in the presence of NaOH and poly(vinylpyrrolidone) (PVP) under

microwave (MW) heating for 10 min. Then, we succeeded in the synthesis of Ag core–Ni

shell nanoparticles, denoted as Ag@Ni, in high yield. The formation of Ag@Ni particles was

confirmed using energy dispersed X-ray spectroscopic (EDS) measurements and selected area

electron diffraction (SAED) patterns. The growth mechanism of Ag@Ni is discussed. The

UV-Vis spectra of Ag@Ni were similar to those of Ni particles.

1. Introduction

Bimetallic nanoparticles have different electronic, optical, catalytic, and magnetic properties from those of individual metals. Therefore much attention has been received for the development of novel synthesis methods for bimetallic nanoparticles and their applications [1-7]. Among various nanoparticles, Ag-Ni bimetallic nanoparticles have attracted great attention due to their technologically important catalytic and magnetic properties [8-16]. Pronounced lattice mismatch, lower surface energy of Ag, and importantly, the complete immiscibility between Ag and Ni make phase segregated core-shell structure the most thermodynamically stable for Ag-Ni stystem [8]. Simulations and calculation (e.g., DFT, global optimization, molecular dynamics, and Monte Carlo simulations) showed that Ni@Ag core-shell structure is thermodynamically favorable [9-12]. Actually, Ni@Ag nanoparticles have been synthesized from Ag_2SO_4 and $Ni(NO_3)_2 \cdot 6H_2O$ by Bala et al. by the foam based protocol using oleic acid as a protecting agent [15]. Chen et al. also synthesized Ni@Ag particles by the successive hydrazine reduction of $NiCl_2$ and $AgNO_3$ in EG without using protective agents or using polyethyleneimine as a protective agent [16].

Since an inverse Ag@Ni structure is thermochemically less stable than Ni@Ag, little study has been carried out except for a recent pioneering work by Zhang et al. [13]. They prepared Ag@Ni using a two-step method. Initially monodispersed Ag seeds were synthesized from $AgNO_3$ using oleylamine (OA) as a weak reductant. Then Ni atoms were controlled to grow upon the Ag seeds by controlling the decomposition of nickel

acetylacetonate in OA. It took more than one day for the preparation of Ag@Ni in this two-step method. The main purpose of their study was controlling magnetic properties of Ni nanoparticles by non-magnetic Ag cores and the formation of Ag@Ni was monitored only by contrast of TEM images and XRD measurements. No EDS and UV–visible (Vis) extinction spectral measurements were carried out, so that definite conclusion about crystal structures and optical properties were not obtained.

We have recently shown that a MW-polyol method is a rapid preparation method of metallic nanoparticles [17]. In the present study, we succeeded in the rapid one-pot synthesis of Ag@Ni particles in high yield using the MW–polyol method. The crystal structure of Ag@Ni particles and optical properties are determined on the basis of transmission electron microscopic (TEM)–EDS data, SAED patterns, and UV–Vis spectra.

2. Experimental section

After 0.08 mM $NiSO_4 \cdot 6H_2O$, $NiCl_2 \cdot 6H_2O$, or $Ni(NO_3)_2 \cdot 6H_2O$ was dissolved in 17.75 mL EG solution in a 100 mL three-necked flask, 2.22 g of PVP (MW:55,000 in terms of monomer units) was added and dissolved. Then, 1 mL of 10 mM $AgNO_3$ in EG and 1.25 mL of 400 mM NaOH were added to the above solution. The reagent solution was heated under MW irradiation (reactor 400W) for 10 min. The final concentrations of Ni salt, $AgNO_3$, PVP, and NaOH were 4 mM, 0.5 mM, 1 M, and 25 mM, respectively. The solution was heated to a

boiling point of EG (198 $^\circ$C) after heating for about 2 min and then kept at this temperature for about 8 min.

For TEM (JEM-2000XS and 2100F; JEOL) observations, samples were prepared by dropping colloidal solutions of the products onto Au grids after centrifugal separation. Extinction spectra of the product solutions were measured using a spectrometer (UV-3600; Shimadzu Corp.) in the UV–Vis region.

3. Results and discussion

When NiSO$_4$·6H$_2$O was used as a reagent, color of solution changed to black before heating. On the other hand, it changed to black after heating when NiCl$_2$·6H$_2$O and Ni(NO$_3$)$_2$·6H$_2$O were used. This indicates that the reduction rate of Ni^{2+} in NiSO$_4$·6H$_2$O is much faster than that in the other two reagents. Figs. 1a-1c depict typical TEM images of product particles obtained from the three reagents. Monodispersed particles with average
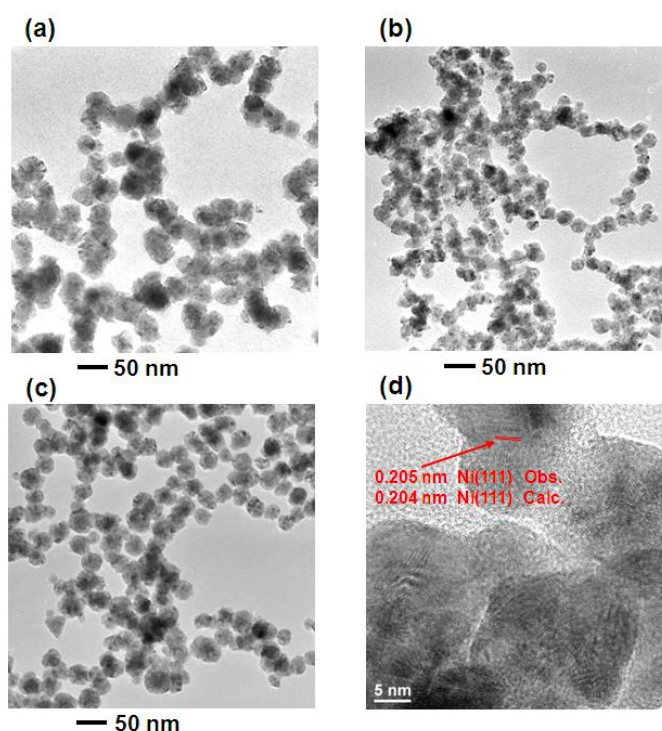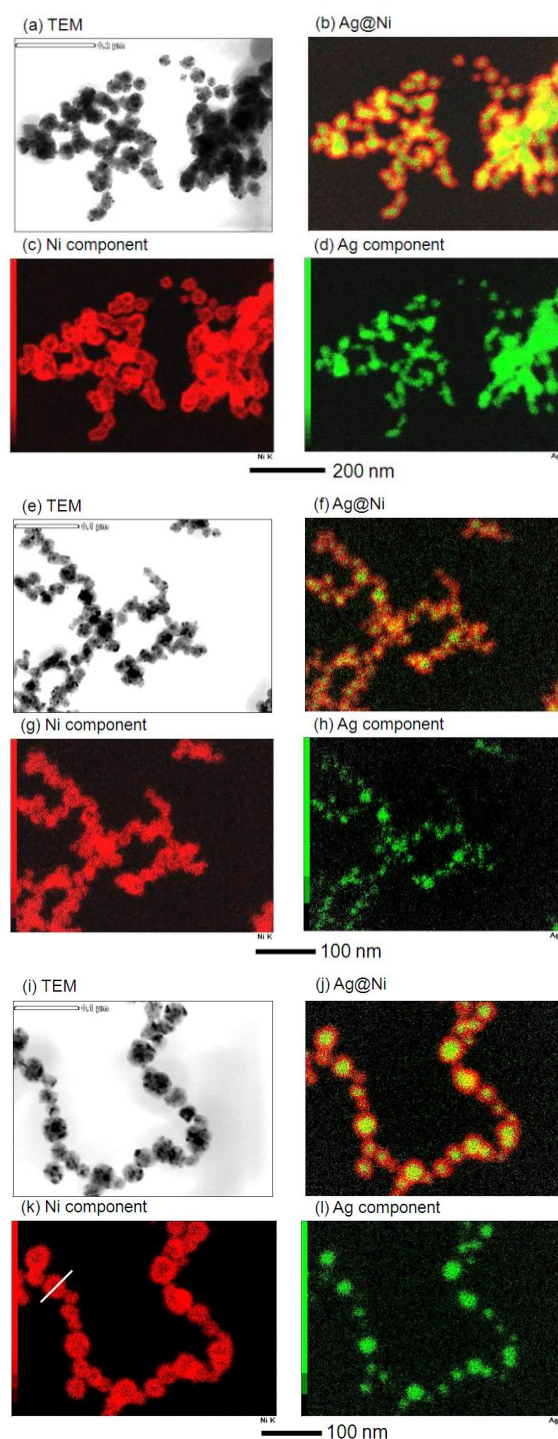

Fig. 1. TEM images of products obtained from mixtures of AgNO$_3$ and (a) NiSO$_4$·6H$_2$O, (b) NiCl$_2$·6H$_2$O, or (c) Ni(NO$_3$)$_2$·6H$_2$O. (d) HR-TEM of products using NiCl$_2$·6H$_2$O.

sizes of 36±6, 22±3, and 33±4 nm were obtained from $NiSO_4 \cdot 6H_2O$, $NiCl_2 \cdot 6H_2O$, or $Ni(NO_3)_2 \cdot 6H_2O$, respectively. Ni(111) facets can be observed in the high resolution (HR)-TEM image (Fig. 1d and Fig. S1 in supplementary data), indicating that Ni nanocrystals exist outside of the product particles.

To obtain more information on the crystal structure, EDS analyses were made (Fig. 2). Although distinguishing between Ag and Ni component from the contrast of TEM images depicted in Figs. 1a–1c, 2a, 2e, and 2i is difficult, EDS data indicate that Ag@Ni core-shell particles are prepared in high yield (100 %). Here the yield was determined by counting the total numbers of Ag@Ni particles and evaluating their fraction in all products. Some particles link together in all cases.

Fig. 3 portrays distributions of the Ag

Fig. 2. TEM images and EDS data of products obtained from mixtures of $AgNO_3$ and (a-d) $NiSO_4 \cdot 6H_2O$, (e-h) $NiCl_2 \cdot 6H_2O$, or (i-l) $Ni(NO_3)_2 \cdot 6H_2O$ under MW heating.

and Ni components along the cross section line of a typical particle shown in Fig. 1k. Similar line analysis data for several particles implied that 12±1.7, 7.5±0.96, and 9.4±1.2 nm Ni shells were overgrown on spherical Ag cores using $NiSO_4·6H_2O$, $NiCl_2·6H_2O$, or $Ni(NO_3)_2·6H_2O$, respectively. The atomic ratios of Ag:Ni were determined to be 18:82, 14:86, and 16:85, respectively for products obtained using $NiSO_4·6H_2O$, $NiCl_2·6H_2O$, or $Ni(NO_3)_2·6H_2O$, respectively. These results

Fig. 3. Distributions of Ag and Ni components in typical Ag@Ni particles along a line shown in Fig. 2k.

Fig. 4. SAED pattern of Ag@Ni particles prepared using $Ni(NO_3)_2·6H_2O$.

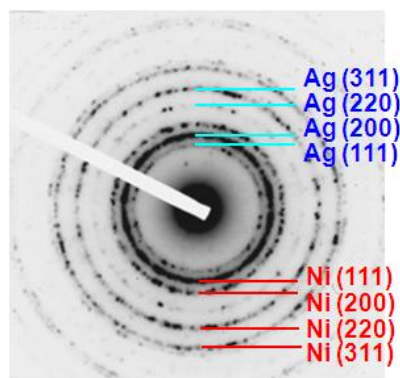imply that the product structures and Ag:Ni atomic ratios were essentially independent of the Ni salt. An advantage of the present method is that monodispersed Ag@Ni particles can be prepared in one pot without using Ag seeds under MW heating for only 10 min.

We have also prepared Ag@Ni particles using a conventional oil-bath heating to examine effects of MW heating. For example, Ag@Ni particles obtained using $Ni(NO_3)_2·6H_2O$ under oil-bath heating (500 W) is shown in Fig. S2 (supplementary data). Although Ag@Ni particles can be prepared under oil-bath heating, it took at least 40 min to prepare Ag@Ni. The average

size of Ag@Ni and thickness of Ni shells were 57±17 and 17±2.3 nm, which were larger than those obtained under MW heating by factors of 1.7 and 1.8, respectively. These results imply that smaller particles having a narrow size distribution could be prepared in a short time under MW irradiation. Uniform heating of the reagent solution gives smaller monodispersed nanoparticles.

Fig. 4 shows a typical SAED pattern of Ag@Ni particle. We could observe many ED spots of (111), (200), (220), and (311) facets of Ag and Ni in SAED patterns. Similar patterns were obtained from the other two Ni reagents. It was therefore concluded that Ag@Ni particles are not amorphous but polycrystals having an fcc type of crystal structure. This finding is consistent with the HR-TEM data, where (111) facets of Ni were clearly observed.

UV–Vis spectra were measured to characterize optical properties and to examine crystal growth of Ag@Ni particles (Fig. 5). For comparison UV–Vis spectra of typical spherical Ag and Ni particles in EG are also shown. Spherical Ag particles give surface plasmon resonance (SPR)
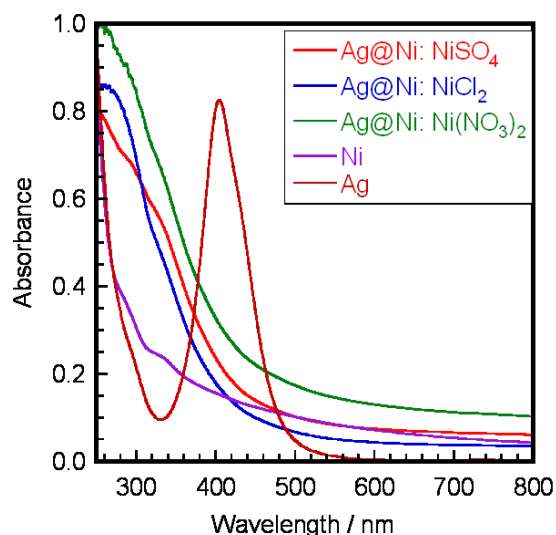
Fig. 5. UV-Vis spectra of Ag@Ni particles prepared from three Ni salts, Ni, and spherical Ag

bands with peaks at ≈400 nm, whereas a weak continuous tail band is observed above 250 nm

from Ni particles. The spectral features of Ni particles are similar to those reported previously [18]. The SPR bands of Ag@Ni are similar to that of Ni particles. On the other hand, it is known that the SPR band of Ni@Ag particles gives a similar SPR band due to Ag shell at $\approx$400 nm [15,16]. These facts imply that the SPR bands of Ag@Ni and Ni@Ag reflect SPR characters of outer shells. This result is different from that of Ag-Cu bimetallic system where both Ag and Cu or their mixed components appear in the SPR bands [6,7,19].

On the basis of TEM–EDS and UV–Vis spectral data, it is reasonable to assume that Ag@Ni is grown through the following mechanism. Under the present fast MW heating, the crystal structure is not determined by thermochemical equilibrium of products but it is controlled kinetic factors such as reduction rates of Ni^{2+} and Ag^+. Since the standard potential of Ni^{2+}/Ni^0 (-0.257 eV) is low, the reduction rate of Ni^{2+} is slow. Therefore, few Ni particles are formed without addition of strong reducing agent NaOH, when Ni salts are reduced in EG in the presence of PVP. On the other hand, since the standard potential of Ag^+/Ag^0 (+0.799 eV) is relatively high, the reduction rate of Ag^+ is fast. Therefore, Ag^+ is reduced to Ag^0 more rapidly than Ni^{2+} and Ag cores are initially formed.

We found that no Ag/Ni alloys were formed in our conditions. One reason is that the reduction rate of Ag^+ is much faster than that of Ni^{2+} at 198 ^{o}C. If Ni^0 particles are formed through the reduction of Ni^{2+}, they are oxidized again through the following spontaneous redox reaction in the presence of Ag^+.

$$2Ag^+ + Ni^0 \rightarrow Ni^{2+} + 2Ag^0 \qquad\qquad (1)$$

This implies that Ni^{2+} ions are reduced after Ag^+ ions are completely reduced to Ag^0. This is

the other reason why Ag/Ni alloys and Ni@Ag particles are not formed from the mixture of

Ag^+ and Ni^{2+}.

It is known that the reduction of Cu^{2+} is enhanced in the presence of silver nanoparticles

[19]. This is due to the cathodic polarization of the Ag particles by electron transfer from

organic radicals generated in the solution and subsequent reduction of Cu^{2+} directly on the

surface of the Ag particles. A similar cathodic polarization of the Ag nanoparticles may occur

in the present system, where some organic radicals and electrons are formed as intermediates

in thermal decomposition of EG [17].
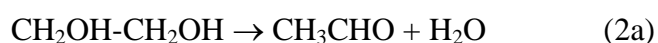
$$CH_2OH\text{-}CH_2OH \rightarrow CH_3CHO + H_2O \qquad (2a)$$

$$2CH_3CHO \rightarrow CH_3COCOCH_3 + 2H^+ + 2e^- \qquad (2b)$$

The cathodic polarization of the Ag particles by electron transfer from organic radicals and by

electron attachment on Ag particles may accelerate reduction of Ni^{2+} on Ag particles. This is

another reason why Ag@Ni particles are preferentially formed from the mixture of Ag^+ and

Ni^{2+}.

4. Conclusions

We succeeded in the fast one-pot synthesis of monodispersed Ag@Ni particles in high

yields from three Ni reagents using a MW-polyol method. Our result gave a new promising technique for the mass production of Ag@Ni particles. Although the core-shell structure of Ag@Ni particles was examined from the contrast of TEM images in a previous study [13], it was definitely confirmed by the TEM-EDS measurements in this study. The optical properties of Ag@Ni were similar to that of Ni nanoparticles, indicating that the shell component determines the optical properties in the Ag-Ni bimetallic system.
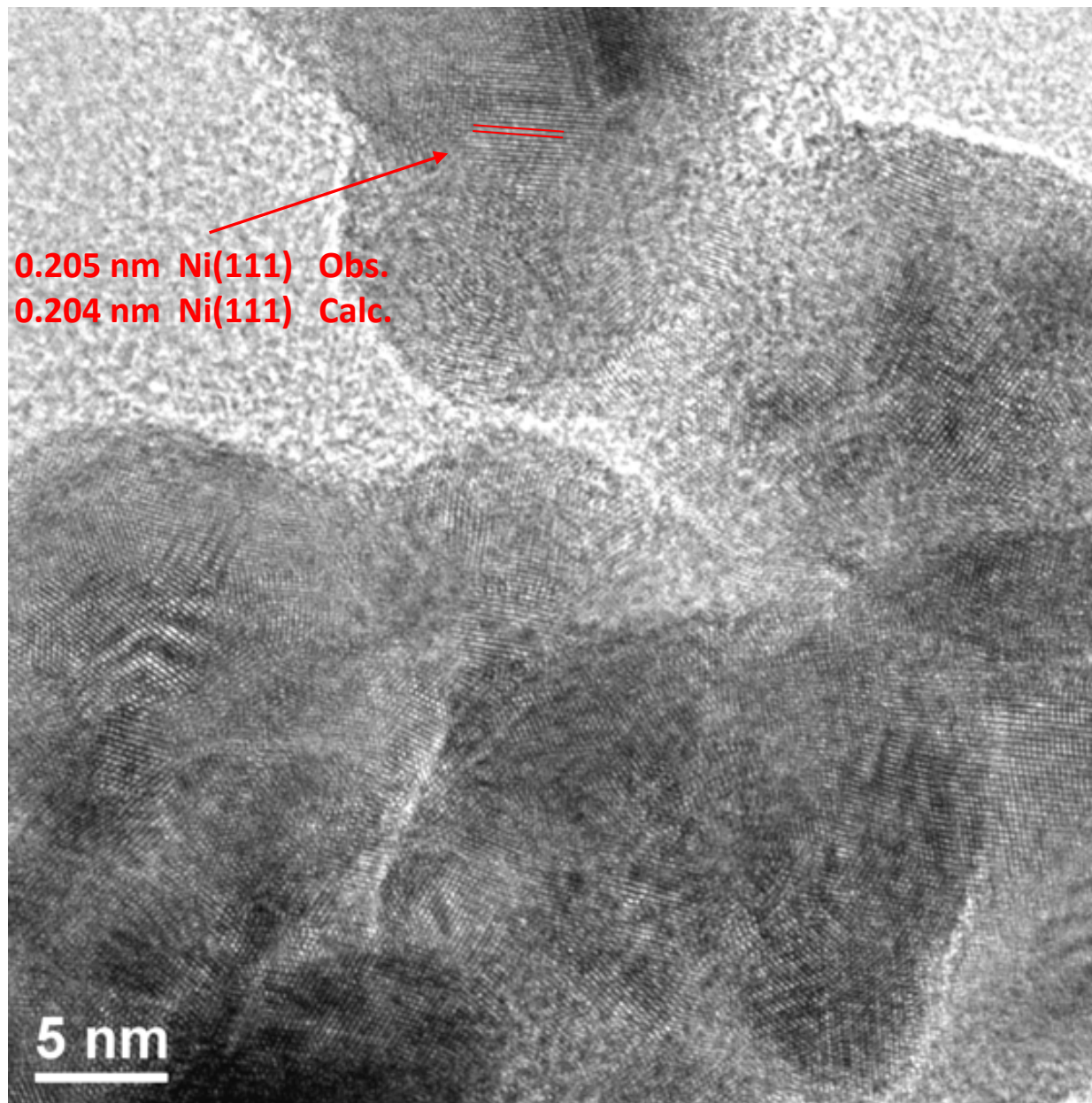
Acknowledgements

References

[1]   Toshima N. Pure Appl Chem 2000;72:317–25.

[2]   Habas S, Lee H, Radmilovic V, Somorjai GA, Yang P. Nature Mater 2007;6:692–7.

[3]   Majo KJ, De C, Obare SO. Plasmonics 2009;4:61–78.

[4]   Tsuji M, Miyamae N, Lim S, Kimura K, Zhang X, Hikino S, Nishio M. Cryst Growth Des 2006;6:1801–7

[5]   Tsuji M, Matsuo R, Jiang P, Miyamae N, Ueyama D, Nishio M, et al. Cryst Growth

        Des 2008;8:2528–36.

[6]   Tsuji M, Hikino S, Sano Y, Horigome M. Chem Lett 2009;38:518–9.

[7]   Tsuji, M, Hikino, S, Tanabe R, Sano Y. Chem Lett 2009;38:860–1.

[8]   Gaudry M, Cottancin E, Pellarin M, Lermé J, Arnaud L, Huntzinger JR, et al. Phys

        Rev B 2003;67:155409 (10 pages).

[9]   Rossi G, Rapallo A, Mottet C, Fortunelli A, Baletto F, Ferrando R. Phys Rev Lett

        2004;93:105503 (10 pages).

[10]   Rapallo A, Rossi G, Ferrando R, Fortunelli A, Curley BC, Lloyd LD et al. J Chem

        Phys 2005;122:194308 (13 pages).

[11]   Harb M, Rabilloud F, Simon D. J Phys Chem A 2007;111:7726–31.

[12]   Calvo F, Cottancin E, Broyer M. Phys Rev B 2008;77:121406 (4 pages).

[13]   Zhang HT, Ding J, Chow GM, Ran M, Yi JB. Chem Mater 2009;21:5222–8.

[14]   Tang C, Li L, Gao H, Li G, Qiua X, Liub J. J Power Sources 2009;188:397–401.

[15]   Bala T, Bhame SD, Joy PA, Prasad BLV, Sastry M. J Mater Chem 2004;14:2941–5.

[16]   Chen DH, Wang SR. Mater Chem Phys 2006;100:468–471.

[17]   Tsuji M, Hashimoto M, Nishizawa Y, Kubokawa M, Tsuji T. Chem Eur J

        2005;11:440–52.

[18]   Tsuji M, Hashimoto M, Tsuji T. Chem Lett 2002;31:1232–3.

[19]   Jiang H, Moon KS, C. P. CP. 10th Int. Symp. Advpack. Mater: Process. Properties and

Interfaces 2005:173–177.

Supplementary data

Expanded HR-TEM image of Fig. 1-d and Ag@Ni prepared under conventional oil-bath

heating are given in supplementary data (http://www.sciencedirect.com).

Fig. S1. Expanded HR-TEM image of **Fig.** 1d.